Application of X-ray Diffraction, Micromagnetic and Hole Drilling Methods for Residual Stress Determination in a Ball Bearing Steel Ring

by C.O.D. Martins, T.R. Strohaecker, A.S. Rocha and T.K. Hirsch

ABSTRACT—A basic understanding of distortion problems requires the analysis of a complete manufacturing process including an almost complete overview of residual stress states in the component during each production step. To reduce the measurement time in the future, three measurements methods (X-ray diffraction, micromagnetic and blind hole drilling methods) have been used to analyze residual stress states in machined AISI 52100 ball bearing rings. X-ray diffraction was used as a state-of-the-art method for machining induced residual stresses with pronounced gradients. The ring exhibited a complex residual stress state with high tensile residual stresses at the surface, a strong gradient in depth, and also showed some variation along the outer circumference due to a superimposition of machining induced residual stresses and effects from the clamping device process. Due to this surface state, micromagnetic signals depend on the analyzing frequency. A calibration of the signals was only possible with the X-ray diffraction data. The results of the three different measurement methods correlate reasonably well.

KEY WORDS—Distortion, residual stresses, ball bearing rings, comparison of measurement techniques

Introduction

The distortion of machine components will occur during manufacturing processes and this is responsible for expensive reworking in martensitic hardened states of ball bearings and gears.[1,2] Among the global parameters such as design, casting, and rolling processes of materials as well as machining and heat treatment of components, all together responsible for distortion problems, the generation and relaxation of residual stresses also can generate distortions during any of these manufacturing steps. A research program has therefore been established to understand and control distortion as a system property of manufacturing processes.[2] Three idealized geometries have been chosen for analysis: ball bearing rings made of a ball bearing steel, and shafts and gears made from a case hardened steel.[1,2] The analysis of residual stress effects on distortion during the manufacture of components requires information about residual stress states far beyond any single spot surface analysis up to a depth of some tenth of a millimeter. More information about residual stress states in a component at optimized time can only be achieved if a number of residual stress analysis methods are taken into account.[3–5] As is known, the determination of residual stress states in the cross-section and along the surface of a whole component requires different measurement methods, which always present advantages and disadvantages. Commonly, X-ray and neutron diffraction, the blind hole drilling method, and the micromagnetic and ultrasonic methods have been applied to engineering components.[4] These techniques are normally chosen according to the given measurement problem and the required number of measurements under aspects of the following parameters:[3,4]

- the nature of the material;
- the type of residual stresses;
- the gradient of residual stresses in the part;
- the geometry of the part and the spot or layers analyzed using the technique chosen;
- the on-site or laboratory environment;
- the type of intervention (destructive or non-destructive method);
- the time and length of the intervention;
- the precision and the reliability of the method;
- the cost of the measurement and the price of the equipment required.

It is easy to see that all of these methods differ from each other concerning the parameters given above. It is further known that macro residual stresses are stresses in a body without external forces, moments and/or temperature gradients.[4,6] At the end of a manufacturing process, residual stresses finally affect the service behavior of components depending on their sign, value, and distribution (see, for example, Hauk,[4] Macherauch and Kloos,[6] and Webster and Ezeilo [7]). As an advantage, compressive residual stresses in surface layers improve the performance of mechanical components against

C.O.D. Martins is a Ph.D. student and T.R. Strohaecker is a Professor, Laboratório de Metalurgia Física, Post-Graduation Program of Mines, Metallurgical and Materials Engineering (PPGEM), Federal University of Rio Grande do Sul (UFRGS), Av. Osvaldo Aranha, 99, r. 610, 90035-190 Porto Alegre, RS, Brazil. A.S. Rocha was a Senior Research Scientist (now a Professor of the Metallurgical Department at UFRGS) and T.K. Hirsch (hirsch@iwt-bremen.de) is Head of the Physical Analysis Division, Stiftung Institut für Werkstofftechnik (IWT), BadGasteiner Str. 328359, Bremen, Germany.

Original manuscript submitted: April 19, 2004.
Final manuscript received: March 31, 2005.
DOI: 10.1177/0014485105055434

external loads and increase the fatigue limit. Consequently, they are of considerable interest and importance for both engineers and scientists.[6]

All the measurement methods still need contonuous improvement and comparisons between one another for a better understanding and application (see, for example, Macherauch and Kloos[6] and Fry[8,9]).

In this paper, we present residual stress analysis results for an engineering component, machined ball bearing rings, measured by X-ray diffraction (XRD), micromagnetic analysis, and the blind hole drilling techniques. It is shown that a better density of information on residual stress states can be obtained and the results are comparable within the restrictions of each method. This will lead to a reduced measurement time. As an example, in this research project more than 5000 residual stress measurements per year are required for all the different geometries after the different manufacturing steps.

Experimental Procedure

The chemical composition of the AISI 52100 steel is C = 0.95, Si = 0.20, Mn = 0.43, P < 0.025, S = 0.007, Cr = 1.50, and Mo = 0.052 mass-%.[10] Basically, the manufacturing process of a ball bearing ring from AISI 52100 steel follows these steps [2]:

1. continuous casting or ingot casting;
2. forging of a ring from a steel bar at 1050–1150 °C;
3. ring rolling process at ≈900 °C;
4. spheroidization process at 750 °C for 8 h;
5. machining of the rings to the final shape;
6. heat treatment (austenitizing at 850 °C for 20 min and quenching in oil);
7. annealing at 170°C for 2 h.

Figure 1 gives the microstructure after the fifth step before the final heat treatment (Fig. 1(a)), and after the final heat treatment, step 7, in the hardened state (Fig. 1(b)). Figure 1(a) shows a typical spheroidized microstructure with globular carbides and around 20 μm grain size. The microstructure of the heat-treated ring is annealed martensite with some 13% retained austenite and spheroidized $(Fe,Cr)_3C$ carbides.

The mechanical properties of this steel in a spheroidized and machined state are: yield strength >500 MPa; ultimate tensile strength >900 MPa; hardness ≅ 20–26 HRC; electric conductivity = $2.86 \times 10^6 \Omega^{-1}$ m^{-1}; relative electric permeability = 80.[10,11] The dimensions of the investigated rings are: external diameter = 145 mm; internal diameter = 133 mm; width = 26 mm.

The XRD residual stress analysis correlates measured elastic strains in a crystal lattice to XRD line shifts via Bragg's law:

$$n\lambda = 2d \sin(\theta). \tag{1}$$

Residual stresses are then calculated using X-ray or macroscopic elastic constants:[4,6]

$$\varepsilon_{\varphi\psi} = {}^1/_2 s_2[\sigma_{11}\cos^2\varphi\sin^2\psi + \sigma_{22}\sin^2\varphi\sin^2\psi + \sigma_{33}\cos^2\psi] + {}^1/_2 s_2[\sigma_{12}\sin 2\varphi\sin^2\psi + \sigma_{13}\cos\varphi\sin^2\psi + \sigma_{23}\sin\varphi\sin^2\psi] + s_1[\sigma_{11}+\sigma_{22}+\sigma_{33}], \tag{2}$$

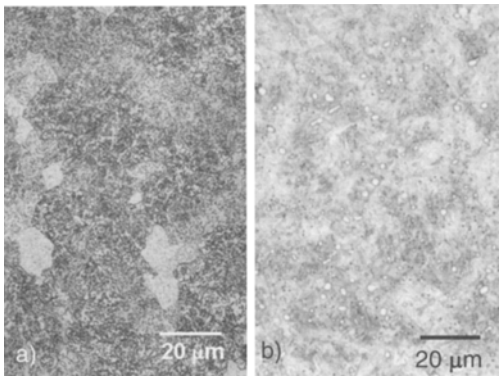

Fig. 1—Microstructure of the ring in the spheroidized state (a) and in the hardened state (b)

where n is the interference order of the crystalline plans, d is the lattice space, θ is the Bragg angle, φ and ψ are the measured angles, and ${}^1/_2 s_2 = (1+\nu)/E$ and $s_1 = -\nu/E$ are the necessary elastic constants. This non-destructive technique is limited to surface layers, where X-rays penetrate a few micrometers depending on the type of radiation and on the absorption of X-rays in a specific material. The analyzed volume in the component therefore depends on the penetration depth and the area of the incident X-ray beam.[4,12]

XRD analysis is a well-established technique. It is applied to obtain localized information from components surface after heat treatment or machining operations.[3,4,6] In the present investigation, an almost complete overview of machining and heat treatment induced residual stresses at the surface and the depth distribution of residual stresses is required to correlate the residual stress state and the distortion found in these rings. No size reduction of the rings was allowed as manufacturing induced residual stresses will relax during a cutting operation. In the first step of the analysis, therefore, 36 residual stress measurements in the tangential direction of the rings were made along the outer circumference. A 10° angular distance between two adjacent points has been chosen, and the measured series started at 0° circumferential direction marked by a hardness indentation. For a complete ring with a 145 mm diameter only this surface was accessible using the setup in the diffractometer (see Figure 2). The 0° position of the ring was further used to mark this position against the clamping system in turning and to mark the ring position in the following heat treatment operations against a position in the furnace chamber.

A typical set of analysis parameters for the XRD residual stress measurement is: CrKα radiation with vanadium filter; analyzed depth, 5 μm; irradiated area, 0.785 mm^2; diffraction line analyzed, {211} lattice plane of α-iron; 2θ range, 151° < 2θ < 60° in steps of 0.1° with a measurement time of 10 s per step. Lattice strains have been analyzed in 15 directions ψ distributed from –45° to 45° equidistanced in $\sin^2\psi$. Reliable residual stress values could be achieved by this procedure using the so-called $\sin^2\psi$ method.[4,6] After the surface measurements, XRD residual stress depth profiles

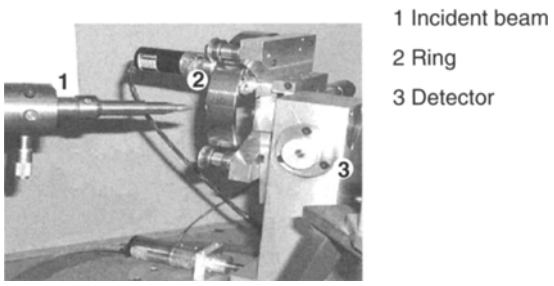

Fig. 2—XRD setup for the residual stress analysis in a ball bearing steel ring: 1, incident beam diaphragm; 2, ball bearing ring; 3, detector and diffracted beam diaphragms/filters

were determinated at 160° and 210° in the circumferential direction of the ball bearing ring. Layer removals were made by electrochemical etching up to 300 μm in depth. The layer removal did not affect residual stress values more than the standard deviation of the measurement due to the low ratio of removed material to the remaining cross-section of the ring.[4]

The residual stress analysis by the micromagnetic method is based on the measurement of the Barkhausen noise and the relative coercitivity. The magnetic flux density in a ferromagnetic material subjected to external time-varying magnetic fields does not change in a strictly continuous way, but rather by small abrupt discontinuous increments. This effect is called Barkhausen jumps.[3,4] These jumps are related to magnetic domain wall movements and the rotation processes occurring in the interior of magnetic domains during the magnetization process.[4,9] If a small analyzing coil is placed between the magnetization coils on a component surface, the change of the magnetization due to domain wall motions can be recorded as an electrical pulse, called Barkhausen noise. The high sensitivity of the magnetic Barkhausen noise to elastic strains has made it an effective tool for investigating deformation in ferromagnetic materials.[4,13–15] The Barkhausen noise is affected by the residual stress states and the microstructure of the material.[4,16] For a positive magnetostrictive ferromagnetic material, the presence of compressive residual stresses reduces the magnetic domain alignment rate in the direction of the external magnetic field and, so far, the intensity of the detected Barkhausen noise. For a tensile stress state, the effect is opposite.[4] The analyzed volume depends on the sensor area in contact with the sample and the analyzing frequency, which can be related to the depth (skin depth δ) according to[4,11]

$$\delta = (\pi f_A C_{electric} \mu_0 \mu_r)^{-0.5} \tag{3}$$

where f_A is the analysis frequency (in Hz), $C_{electric}$ is the electrical conductivity (in Ω^{-1} m^{-1}), μ_0 is the vacuum magnetic permeability ($4\pi \times 10^{-7}$ Hm^{-1}), and μ_r is the material's magnetic permeability.[3,4,11] Micromagnetic measurements were executed with Ferrotest Dur III equipment (manufacturer: Tiede) with a special sensor developed for the geometry of the ring. The magnetization was always performed in the tangential direction, and the results so far can be directly correlated to XRD results. At the outer circumference of the rings, 36 measurement points have been set at angles of former XRD measurements. Two analyzing frequencies of 0.4 and 10 MHz were used to achieve a penetration depth

Fig. 3—View of the Ferrotest Dur III equipment and setup for the residual stress analysis using the micromagnetic method

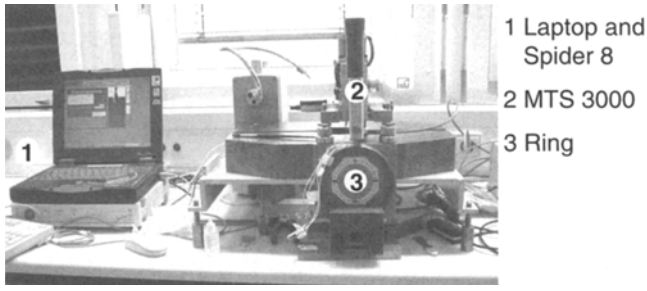

Fig. 4—View of the MTS 3000 equipment for the residual stress analysis using the hole drilling method

similar to X-rays (around 10 μm with the 10 MHz filter) and a significant higher depth of 52 μm with the 0.4 MHz filter. The other measurement parameters are: magnetic field intensity, 100 A cm^{-1}; magnetic field frequency, 100 Hz; amplification, 30 dB for the 10 MHz frequency and 10 dB for the 0.4 MHz frequency; sensor area, 7 mm^2. Figure 3 shows the equipment configuration for the residual stress analysis using the micromagnetic method.

The micromagnetic analysis is an indirect method; a calibration procedure is necessary to obtain the relation between measured signals and residual stress values. This calibration can be carried out via a mechanical tensile/compression test or by residual stress analysis with XRD and the hole drilling method.[4] In this work, the micromagnetic calibration was performed with the XRD residual stress data.

In the blind hole drilling residual stress measurement method, a small hole is drilled into the component and a special strain gage rosette or an optic sensor records the relieved strains. During the drilling process, the strain gage rosette records the strains for each preset depth in three known directions ($\varepsilon_1, \varepsilon_2, \varepsilon_3$). With these strain data, principal residual stresses (σ_{max}, σ_{min}) and principal directions can be calculated using[3,9,11,17]

$$\sigma_{max}, \sigma_{min} = (\varepsilon_3 - \varepsilon_1)/4A \pm [(\varepsilon_3 - \varepsilon_1)^2 + (\varepsilon_3 + \varepsilon_1 - 2\varepsilon_2)^2]^{1/2}/4B. \tag{4}$$

The calibration constants (A and B) can be obtained by a mechanical test or by finite element method simulation. Normally, they are given in standard tables.

As more than one possibility of calculation is available in the literature, only one set of equations is given in eq (4).[17] The hole drilling measurement was made with the MTS 3000 equipment.[17]

The instrument software also offers the possibility to choose the depth increments during drilling. As significant

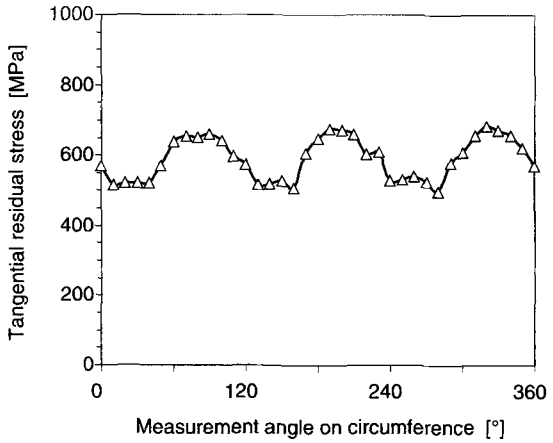

Fig. 5—XRD surface residual stresses in the tangential direction as a function of the measurement angle around the outer circumference of the ring

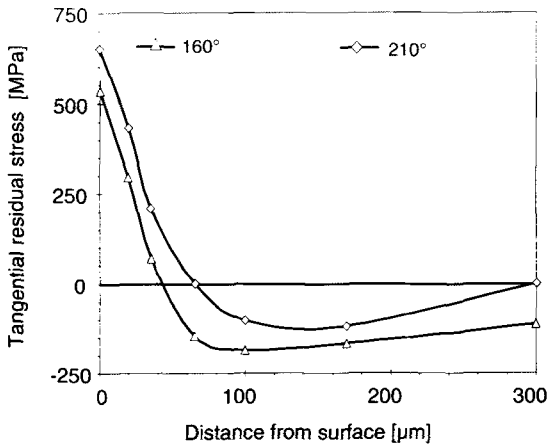

Fig. 6—XRD tangential residual stresses as a function of the distance from the surface for angular positions 160° and 210°

gradients of machining induced residual stresses are expected, a high density of information should be received from near-surface layers. The instrumental setup can be seen in Figure 4. The hole diameter (D_0) was 1.8 mm and the maximum analyzed depth (Z) was 1 mm. Z depends on the strain gage size, which is normally 40% of its diameter (D).[8] As in many other investigations, a strain gage type MM EA–0,62RE–120 was used. Information on geometry and the application of strain gage rosettes are described in the literature.[3,8] Two holes were drilled at 0° and 140° angular positions on the ring. Other parameters for these fully computerized measurements are the feed rate of the drill (0.07 mm min^{-1}) and the end mill diameter (1.6 mm). The surface area analyzed by this method was 2.54 mm^2. The analyzed surface area per measurement is therefore in between that for XRD measurements (0.78 mm^2, irradiated area) and that for the residual stress analysis with the micromagnetic method (7.07 mm^2, sensor area). The analyzed depth of 1 mm is far higher compared to the other methods. Figure 4 shows a view of the equipment configuration during these experimental tests.

35 depth increment have been chosen where the depth distribution can be associated with the following equation

$$Z_n = 8 \times 10^{-4} N^2 + 2.86 \times 10^{-2} N + 3 \times 10^{-4} \quad (5)$$

where N is the increment number and Z_n is the depth. Residual stresses are calculated with the HBM MTS 3000 software. Measured strain data were fitted by a polynomial function and residual stresses have been calculated by the Schajer integral method, which gives an optimum effect in reduced experimental scatter.[17]

Results

The following figures give the experimental results for one ball bearing ring in the machined state. These rings have been machined with titanium nitride coated cemented carbide cutting tools (HC K10 TiN), a depth of cut of 1 mm at a cutting speed of 240 m min^{-1} as a standard set of parameters with 3% emulsion as a coolant. The feed rate was 0.4 mm per revolution. Details of the machining process can be found in Brinksmeier et al.[18–20] and Stölter et al.[21] The turning direction is equal to the tangential direction of the ring. Figure 5 gives machining induced residual stresses as a function of the measurement position (in degrees) around the circumference and Fig. 6 shows residual stress depth distributions at two angular positions. The results in Figs. 5 and 6 have been obtained by XRD.

Typical residual stress distributions are found after turning (Figs. 5 and 6) using three-point clamping segments (each one covers 120°).[18,21] The presence of tensile residual stresses at the surface can be associated with a pronounced thermal–mechanical impact in surface layers superimposing effects from pure plastic deformation. The external distributed load from the three segments for simplification is concentrated in three points, at angles of 30°, 150°, and 270°, against the zero degree orientation of the ring. These clamping stresses in three points are released after withdrawing the ring from the machine and reduce the machining induced residual stress level in the surface partially, as indicated in Fig. 5. Figure 6 proves that these tensile residual stresses occur only in a shallow layer of 40–70 µm thickness. For depths higher than about 70 µm, compressive residual stresses of –100 to –200 MPa are measured. The normal forces of the tool introduce contact stresses into the material. If these exceed the yield strength, plastic deformation below the surface will result in compressive residual stresses. Finally, the machining induced residual stresses at higher distances from the surface decrease towards zero, as expected.[22] Before machining, the spheroidization process with a slow cooling resulted in some compressive residual stresses of –300 MPa in a 300 µm thick layer at both surfaces and in equilibrium tensile stresses of 30 MPa in the rest of the cross-section with 5.4 mm thickness. Neutron diffraction measurements in machined rings additionally proved that residual stresses in the center of the ring do not exceed 30 MPa. Together with the data in Fig. 6, this is in agreement with the equilibrium of forces and moments in a radial cross-section.[23] The depth profiles of residual stresses also are affected by the clamping stresses, as can be seen in Fig. 6 from the two displayed distributions. This again supports the fact that the machining process only is the responsible factor and a superimposition with an existing residual stress field can almost be excluded.

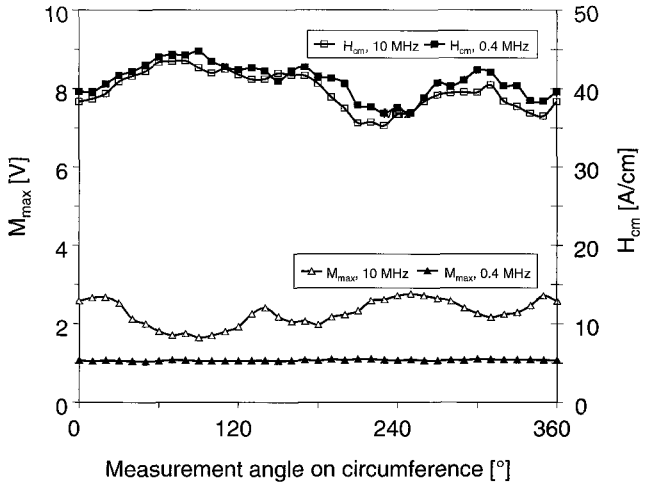

Fig. 7—Amplitude of Barkhausen noise, $M_{\max}$, and the relative coercitivity, H_{cm}, as a function of the measurement angle

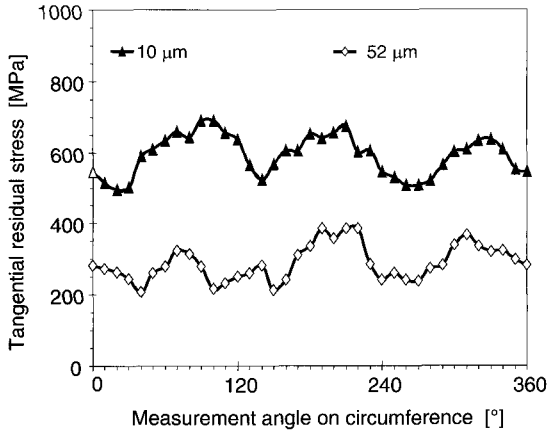

Fig. 8—Residual stresses calculated with eqs (7) and (8) (micromagnetic measurements)

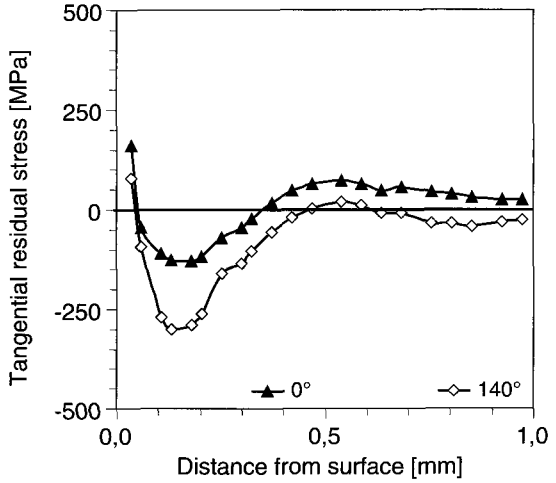

Fig. 9—Measured strain from the hole drilling method for holes at angular positions of 0° and 140°

Figure 7 gives results of the micromagnetic measurements. The maximum intensity of the Barkhausen signal ($M_{\max}$) and the coercitivity (H_{cm}) for the 10 MHz analyzing frequency ($1.5 < M_{\max} < 3$ V) show distributions which are quite similar to XRD results. The Barkhausen noise signal remains constant at around 1 V for the 0.4 MHz analyzing frequency with the significant higher penetration depth.

A calibration procedure was accomplished using a machined tensile test specimen loaded stepwise with defined elastic strains. Measurements of the Barkhausen noise signal and the coercitivity were executed after each loading step. The comparison of yield strength values for the material (see the "Experimental Procedure" section) and surface residual stress values in Fig. 6 immediately clarifies that an exact calibration is impossible, because yielding would occur in the tensile tests for load stresses as high as the tensile residual stresses. An extrapolation of load stresses, Barkhausen noise signal, and relative coercitivity to higher stress values is not allowed due to the microstructural changes after yielding.

It was also impossible to generate the same amount of residual stresses and the same microstructural properties in a flat tensile test specimen. As is often done, finally only a calibration of micromagnetic data with X-ray data was possible. The calibration was performed by using only five randomly distributed XRD residual stress values and a multiple linear regression software.[4] Residual stresses calculated by this method (σ_{MM}) as a function of $M_{\max}$ and H_{cm}, are given by the following equations:

$$\sigma_{MM}(10\,\text{MHz}) = 2091 - 261.36 M_{\max}(10\,\text{MHz}) - 22.75 H_{cm}(10\,\text{MHz}) \quad (6)$$

$$\sigma_{MM}(0.4\,\text{MHz}) = -217.315 - 1064.87 M_{\max}(0.4\,\text{MHz}) - 22.381 H_{cm}(0.4\,\text{MHz}). \quad (7)$$

Using these equations, residual stress distributions over the circumference of the ring are plotted in Fig. 8 for two analyzing frequencies.

With the frequency of 10 MHz, the correlation with XRD residual stresses is good, as expected (compare Fig. 6 with Fig. 8). Applying eq (8) for the frequency of 0.4 MHz, an almost similar distribution of residual stresses can be seen in Fig. 8. The results are however shifted to lower tensile values of around 300 MPa.

Figure 9 shows the measured strain distributions for two holes drilled at the 0° and 140° angular positions. ε_T was measured in the tangential direction, ε_{45} at 45° for this direction, and ε_A in the axial direction of the ring. Note that for both holes the relieved strains increase to 0.5 mm in depth, especially in the tangential direction. This can be an indicative of a large difference in the residual stress depth profile. Despite the fact that holes in the blind hole drilling method have been drilled to a depth of 2 mm, the calculation of residual stresses was limited to 50% of the total depth.[3] No major sensitivity to relieved strains at depths higher than 1 mm can be seen from Fig. 9. Figure 10 displays the results of the residual stress calculations.

The principal direction for these measurements was found to deviate between only 1° and 3° from the tangential

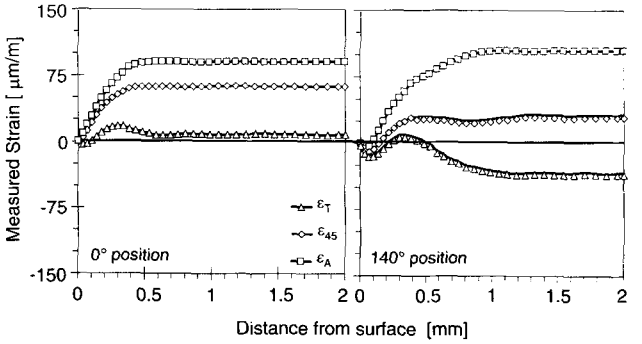

Fig. 10—Tangential residual stresses obtained with the hole drilling method, calculated by the Schajer integral method, for holes at angular positions of 0° and 140°

direction, which is the turning direction. As expected from XRD results, residual stresses in Fig. 6 decrease from tensile residual stresses at the surface to compressive ones at a depth of less than 0.1–0.3 mm. At higher depth (higher than 0.3 mm) some tensile residual stresses of about 50 MPa are observed, which decrease towards zero for distances from the surface higher than 0.5 mm.

Discussion

In this paper we report on the results of residual stress state evaluation in a typical engineering component. Any basic understanding of distortion problems and possible solutions to minimize this problem require the analysis of a complete manufacturing process. This includes a complete overview of residual stress states in the component during each production step, as far as is possible with given limitations in time.[1,2] Results are reported here from three different measurement methods, each with specific advantages and disadvantages. A comparison of different residual stress measurement methods was the object of several round-robin tests between different laboratories, each an expert in a single measurement method.[24,25] The advantage of the present investigation is that all the different measurement methods have been executed in one laboratory with one specimen only. As a consequence, some of the possible errors are minimized. The presentation concentrated on residual stresses in the tangential direction only, as results from different methods are demonstrated rather than a complete description of a residual stress field. Although the term residual stress measurement has come into common use, it is important to remember that residual stresses are not directly measured, but they are determined from the measurement of some intrinsic material properties.[12] The XRD method is based on the measurement of strains in the crystal lattice, the micromagnetic method on Barkhausen jumps and relative coercitivity measurements, and the blind hole drilling method on relieved strains after each step of the drilling process.[3–5] The XRD method is non-destructive for surface measurements and applied in laboratory and field measurements. XRD residual stress measurements are executed with small analyzed volumes, and therefore give only localized information at a small depth. To consider residual stress states in a whole component requires time-consuming multiple measurement spots and layer removal for depth profiling. However, it is the state-of-the-art method for machining induced residual stresses with pronounced gradients. As Fig. 5 proves, XRD measurements give an overview of surface residual stresses in the component. The measurement time was more than 24 h. With the low penetration depth of X-rays, strong gradients of residual stresses in a 50 µm thick layer can be detected in an excellent manner, if layer removal is small in each case (see Fig. 6). Information on residual stress states over the complete surface of a whole component is available only in a few cases (see, for example, Hauk[4]). The superimposition of the turning process itself (elastic–plastic deformation at increased temperatures) and the clamping system have been revealed only by this high density of information.[18–22] The inhomogeneous distribution of residual stresses along the surface coincides with a distortion maximum of several tenths of a micrometer, also 120° apart. It is further known that annealing of these rings results in an even bigger distortion due to the inhomogeneous relaxation of residual stresses.[26] This clearly demonstrates the importance of analyzing distortion and residual stresses in each manufacturing step, together with preceding and succeeding steps.

Speeding up the process, micromagnetic measurements in ferromagnetic materials are suitable and have been applied successfully.[3,4] With the newest equipment, a multiparameter analysis is capable of computing residual stress values directly from more than two measured micromagnetic properties. In general, the method needs a calibration procedure for each of the analyzed microstructures.[4] As in the present case, it is sometimes difficult to produce a tensile test specimen for calibration with the same surface state and the same high tensile residual stresses, e.g., after turning. As a consequence, some XRD data have to be used for the correlation of micromagnetic signals and residual stresses. Due to the strong residual stress gradient, the analyzing frequency is also an important factor. Figures 7 and 8 demonstrate that only the highest analyzing frequency is able to detect the surface residual stress distribution along the tangential direction with a sufficient reliability. In this case, the highest values of dangerous tensile residual stresses at the surface will not be detected if only low analyzing frequencies are applied during the measurement. The total number of 36 measurements, and even higher numbers in the future, on the other hand required only 1 h of measurement time.

The blind hole drilling method is also a commonly used method for residual stress characterization. It is cheap, fast, and can be considered as a semidestructive method, if the volume removed can be tolerated or repaired. Its precision depends on equipment adjustments, strain gage type used, and on the calculation method (see, for example, Fry[9]). The volume analyzed is proportional to the volume of the material removed, where the area of the surface is similar to the hole area. So far, this method would be very time-consuming for the detection of information along the circumference as required for the measurement problem in this investigation. However, only with the blind hole drilling method can a depth profile of residual stresses be achieved for up to 1 mm surface distance in a time less than 1 h (strain gage application time included).

The results of the three different measurement methods correlate reasonably well in spite of the fact that the turned ring exhibited a rather complex residual stress state. As shown, residual stresses not only vary in depth with a strong

gradient, but also show some variation along the outer circumference of the ring. This is due to the superimposition of machining induced residual stresses and effects from the clamping.[19–21] In a homogeneous isotropic material without major texture, residual stresses determined by XRD give reliable and exact information after machining or heat treatment processes. For the micromagnetic data, at lower frequencies, always an integral residual stress value in a thicker surface layer will be examined. If the sensor and the data evaluation instrument are able to analyze at frequencies as high as 10 MHz, data from a 10 μm thick surface layer can be recorded and correlated with XRD results.

An integral of the depth profile in Fig. 8 made to a depth of 50 μm gives values of 300 MPa tensile residual stresses. This corresponds fairly well with results obtained from micromagnetic measurement with 0.4 MHz analyzing frequency.

The comparison of XRD and blind hole drilling surface residual stresses can also be understood from the different analyzed volumes. The first hole depth was at 30 μm, which according to the sharp residual stress gradient (Fig. 6) should result in a lower integral value of 300–400 MPa, as shown in Fig. 10. Lower residual stress values such as those determined by XRD are the consequence. Also, the interpolation of measurement results to the very surface made by any hole drilling calculation software can cause differences to the XRD data. The blind hole method again proved that residual stresses in the interior of the ring seem to be quite low. This can be understood from the soft-annealing process and the fairly slow cooling before machining.

Conclusions

A basic understanding of distortion problems requires the analysis of a complete manufacturing process including an almost complete overview of residual stress states in the component during each production step. To reduce the measurement time, three measurement methods have been used to analyze residual stress states in machined ball bearing rings. XRD was used as a state-of-the-art method for machining induced residual stresses with pronounced gradients. The ring exhibited a complex residual stress state with high tensile residual stresses at the surface, a strong gradient in depth, and it also showed some variation along the outer circumference due to a superimposition of machining induced residual stresses and effects from the clamping systen during the machining process. Due to this surface state, micromagnetic signals depend on the analyzing frequency. A calibration of the signals was only possible with the XRD data. The results of the three different measurement methods correlate reasonably well, if the specific analyzing differences in the methods are considered.

Acknowledgments

The present work is a part of an ongoing research program of the German Science Foundation DFG (Deutsche Forschungsgemeinschaft) SFB–570 "Distortion Engineering". The authors would like to thank the DFG for their support. CODM and TRS wish to express their gratitude to CNPq–Brazil for their support.

References

1. Thoben, K.D., Luebben, Th., Clausen, B., Prinz, C., Schulz, A., Rentsch, R., Kusmierz, R., Nowag, L., Surm, H., Frerichs, F., Hunkel, M., Klein, D., and Mayr, P., "Distortion Engineering—Eine systemorientierte Betrachtung des Bauteilverzugs," Haerterei-Technische Mitteilungen, **57** (4), S. 276–282 (2002).

2. Hoffmann, F., Kessler, O., Lübben, Th., and Mayr, P., "Distortion Engineering – Distortion Control During the Production Process," Heat Treatment of Metals, **2**, 27–30 (2004).

3. Lu, J., Handbook of Measurement of Residual Stresses, SEM, Bethel, CT (1996).

4. Hauk, V., Structural and Residual Stress Analysis by Non-destructive Methods, Elsevier, Amsterdam (1997).

5. Ruud C., "Measurement of Residual Stresses," Handbook of Residual Stress and Deformation, ASM, Materials Park, OH, 99–117 (2002).

6. Macherauch, E. and Kloos, K., "Origin, Measurement and Evaluation of Residual Stresses," Residual Stresses in Science and Technology, **1**, 3–27 (1987).

7. Webster, G. and Ezeilo, N., "Residual Stress Distributions and Their Influence on Fatigue Lifetimes," International Journal of Fatigue, **23**, 375–383 (2001).

8. Fry, T., Measurement Good Practice Guide No. 52, National Physical Laboratory, UK (2000).

9. Fry, T., Measurement Good Practice Guide No. 53, National Physical Laboratory, UK (2000).

10. Lampman, St., Zone, T. eds. "Properties and Selection, Iron Steels and High Performance Alloys," Metals Handbook, Vol. 1, 10th edition, ASM, Materials Park, OH, 152 (1990).

11. Martins, C.O.D., "Comparação entre Técnicas de Análise de Tensões Residuais em Anéis para Rolamentos," Master's Thesis, PPGEM, UFRGS, Brazil (2004).

12. Prevey, P.S., "X-ray Diffraction Residual Stress Techniques," Metals Handbook, ASM, Materials Park, OH, 380–392 (1986).

13. Withers, P. and Bhadeshia, K., "Residual Stress: Part 1," Materials Science and Technology, **17**, 355–365 (2001).

14. Withers, P. and Bhadeshia, K., "Residual Stress: Part 2," Materials Science and Technology, **17**, 366–375 (2001).

15. Stefanita, C.G., Atherton, D.L., and Claphan, L., "Plastic Versus Elastic Deformation Effects on Magnetic Barkhausen Noise in Steel," Acta Materialia, **48**, 3545–3551 (2000).

16. Karpuschewski, B. and Oberbeck-Sprintig, I., Residual Stress Determination of Ferromagnetic Sheets, ICRS5, Sweden, 1145–1149 (1997).

17. MTS 3000, Equipment Manual, HBM Company, Darmstadt, Germany (2002).

18. Brinksmeier, E. et al., "Residual Stresses—Measurement and Causes in Machining Processes," CIRP Annals, **31**, 491–510 (1982).

19. Brinksmeier, E. et al., "Simulation der Werkstückdeformation beim Spanen von Ringen," Haerterei-Technische Mitteilungen, **58**, 271–275 (2003).

20. Brinksmeier, E. et al., "Einfluss der Drehbearbeitung auf den Verzug von 100Cr6–Ringen," Haerterei-Technische Mitteilungen, **58**, 266–270 (2003).

21. Stölter, J., Nowag, L., Rocha, A., Walter, A., Brinksmeier, E., and Hirsch, T., "Einfluss der Maschinenstellgrößen auf die Eigenspannungszustaende beim Drehen von Waelzlagerringen," Haerterei-Technische Mitteilungen, **59**, 169–175 (2004).

22. Hirsch, T., "Eigenspannungen in Fertigungsprozessen," Haerterei-Technische Mitteilungen, **58**, 110–126 (2003).

23. Hirsch, T., Rocha, A., Martins, C., and Rosendo, T., "Vergleich verschiedener Eigenspannungs-messmethoden an den Geometrien des SFB 570—Distortion Engineering," Haerterei-Technische Mitteilungen, awaiting publication (2005).

24. Flaman, M.T. and Herring, J.A., "SEM/ASTM Round-robin Residual Stress Measurement Study—Phase I 304 Stainless Steel Specimens," Experimental Techniques, **12**, 23–25 (1988).

25. Hauk, V. and Kockelmann, H., "Eigenspannungszustand der Laufflaeche einer Eisenbahnschiene," Haerterei-Technische Mitteilungen, **49**, 340–352 (1994).

26. Volkmuth, J., Sjöblom, U., Slycke, J., and Thuvander, A., "Effect of Uneven Residual Stresses on Dimensional Changes and Variations of Through Hardening Bearing Steel Rings," Proceedings of the 20th ASM Heat Treating Society Conference, ASM International, Materials Park, OH, 173–195 (2001).